Molecular Biology and Evolution, 2026, 43, 1–7
https://doi.org/10.1093/molbev/msag101
Published: 15 April 2026
Brief communications

MBE OXFORD

Degeneration and adaptive evolution of digits in ratite birds

Wen Kang [1,2], **Günter Wagner** [3,4,5,6], **Qi Zhou** [1,2,7,8]*

[1]Center for Reproductive Medicine, Second Affiliated Hospital of Zhejiang University School of Medicine, Life Sciences Institute, Zhejiang University, Hangzhou, Zhejiang 310058, China
[2]Center for Evolutionary & Organismal Biology, Zhejiang University, Hangzhou 310058, China
[3]Department of Ecology and Evolutionary Biology, Yale University, New Haven, CT, USA
[4]Yale Systems Biology Institute, Yale University, New Haven, CT, USA
[5]Department of Evolutionary Biology, University of Vienna, Vienna, Austria
[6]Hagler Institute for Advanced Study, Texas A&M University, College Station, TX, USA
[7]Zhejiang Provincial Key Laboratory for Cancer Molecular Cell Biology, Life Sciences Institute, Zhejiang University, Hangzhou, Zhejiang 310058, China
[8]State Key Laboratory of Transvascular Implantation Devices, Hangzhou 310058, China
***Corresponding author:** E-mail: zhouqi1982@zju.edu.cn.
Associate editor: Patricia Wittkopp

Abstract

The amniote digits have undergone recurrent modifications, with the diversified molecular mechanisms more studied among mammals than reptiles. Here we focus on the emu wings and ostrich feet, both of which experienced species-specific digit changes driven respectively by secondary flight loss and adaptation to running. By comparing their digit transcriptomes to those of chicken and alligator, we identified different gene networks in skeleton/muscle development responsible for the degenerated digits in archosaur ancestors and emu, but those in epidermal development for the load-bearing digit of ostrich. These results provide new clues for developmental programs of different cell types between different digits, on which natural selection can convergently operate.

Keywords digit evolution, ratites, digit development

Introduction

Most extant tetrapods have a pentadactyl ground state of digits with repeated modifications to the number and morphology of certain digits, as a result of species-specific adaptation for different locomotive purposes. The molecular mechanism underlying the reduction or loss of individual digits is informative for the digit specification and evolution program, and has been elucidated in various mammals. It involves either reduced expression of the receptor of limb-patterning morphogen *Shh*, *Ptch1* early in the limb bud of cattle and pig; or involves, during later stages, increased expression of apoptosis-associated genes (e.g. *Bmp4*) in certain digits of jerboa, horse, and camel (Cooper et al. 2014). Little is known about how some digits became lost in other tetrapods.

Birds comprise a great model for studying digit evolution and development with their great diversity of digit number and configuration (different numbers of toes facing forward/backward between species) (Raikow 1985; Botelho et al. 2014; Botelho et al. 2015), likely because of functional specialization between wings vs. feet (Abourachid 2006). Most birds have 3 wing digits, while the emu (*Dromaius novaehollandiae*) further completely loses the other 2 vestigial digits during development due to secondary loss of flight. Previous works reported decreased expression of *fgf10* (Young et al. 2019), and increased expression of an cardiac transcriptional factor *Nkx2.5* (Farlie et al. 2017) likely account for the heterochronic and attenuated development of the emu limb bud. But it is unknown what genes are associated with digit loss at later development. The ostrich (*Struthio camelus*), a distinct ratite lineage that lost flight independently of the emu, retains the 3 wing digits for sexual display (Feduccia and Nowicki 2002; Farlie et al. 2017), but develops 5 digits in embryonic feet and loses digits 1, 2, 5 during later development. Its retained hindlimb digit 3 is the major load-bearing digit (Schaller et al. 2011), and is supposed to be highly adapted for fast and long-distance running. Therefore, ratites offer opportunities for dissecting mechanisms of both functional degeneration and adaptive evolution of individual digits in response to the transition of locomotive modes.

Results and discussion

To identify the candidate genes responsible for developmental changes of ratite digits, we collected transcriptomes from individual

Received: October 14, 2025. **Revised:** March 9, 2026. **Accepted:** March 30, 2026

developing digits of 2 ratites (emu and ostrich) and chicken (*Gallus gallus*) (without those modifications mentioned above), together with 2 pentadactyl reptiles (Siamese crocodile (*Crocodylus siamensis*) and Chinese softshell turtle (*Pelodiscus sinensis*)) as outgroups, sampled separately from forelimbs and hindlimbs at 2 developmental stages ((Wang et al. 2011), see Materials and Methods). Although the 2 emu wing digits and the 3 ostrich hindlimb digits, as well as crocodile hindlimb digit 5, lack bony structures in the adult, they proceed through a cartilaginous stage during embryogenesis, as confirmed by Alcian blue staining (Fig. 1, Figure S1). And as the identity of 3 avian wing digits remains a subject of debate, the embryological and morphological evidence support most birds' digit identity as a 2-3-4 identity (Kundrát 2009; de Bakker et al. 2013; de Bakker et al. 2021), while the transcriptomic analyses reveal molecular signatures of a 1-3-4 identity (Stewart et al. 2019). Given the transcriptomic nature of this study, we follow the latter nomenclature (thumb, middle, and ring finger).

To investigate the molecular mechanisms of digit loss or modification, we focused on the candidate genes showing significant gene expression changes through 2 complementary approaches. First, we identified molecular fingerprint genes (MFGs)—genes that are preferentially up- or downregulated in a given digit within the same species in at least one of the 2 sampled stages (Materials and Methods). Second, we identified the genes showing fast change in expression (FCEGs) relative to homologous digits in other species in at least 1 of the 2 sampled stages (Materials and Methods; Table S1). Collectively, the union of these 2 sets allowed us to prioritize candidate genes potentially associated with digit degeneration or adaptive modification.

While most of these digits have undergone changes after the species divergence from the Archosauria ancestor, the hindlimb digit 5 (HD5) could have evolved degeneration either in the ancestor of Archosauria or independently in ostriches and crocodiles. It is absent in all adult birds but has a vestigial form in embryos of ostrich and crocodiles, after its positional identity is specified (de Bakker et al. 2013) (Fig. 1). To distinguish the 2 scenarios, we examined the MFGs and FCEGs genes (termed together "candidate genes' hereafter) in HD5s of the 2 species and found that 70% and 77% of the crocodile and the ostrich orthologous candidate genes are shared. This suggests that the HD5 was present and started to degenerate in the Archosauria stem lineage, and it further became completely lost in most dinosaurs and modern birds (Gauthier 1986; Gatesy 1995). The candidate genes of degenerating ostrich and crocodile HD5s are enriched (hypergeometric test, $P < 0.05$) for Gene Ontology (GO) terms of skeleton, muscle, and skin development (Fig. 2b, Table S2). Particularly, genes of skeleton development all show downregulation of expression relative to other digits: the upstream chondrocyte differentiation genes *Sox9*, *Runx2*, and *Acan* are all downregulated in ostrich and crocodile HD5s, as well as in the ostrich HD1 relative to other digits of the same and homologous digits of related species (Fig. 2a, Figure S2). Mouse mutants of these genes show many skeletal disorders, including shortened

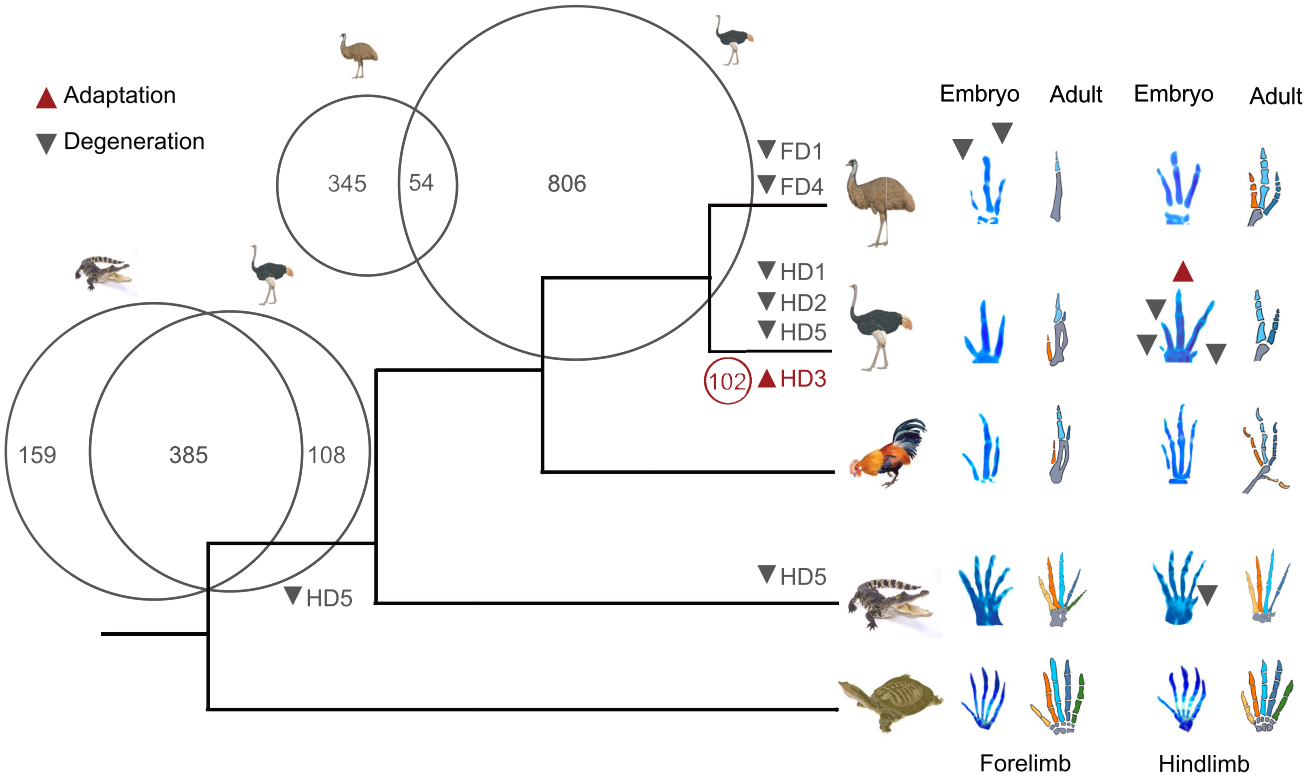

Figure 1 Degeneration and adaptive evolution of individual Archosaur digits. We studied 2 ratites (emu and ostrich) and chicken, together with 2 pentadactyl reptiles (Siamese crocodile and Chinese softshell turtle) for their individual developing digit in forelimbs and hindlimbs. Cartilage staining with Alcian blue of each collected digit sample is shown in the right panel, with the degenerating digits and putatively adaptively evolving digit marked by black and red arrows. The Venn diagrams on the branches show the overlapped candidate genes for the degenerating HD5 of ostrich and crocodile, and also the number of overlapped candidate genes responsible for all the degenerating emu forelimb digits I and IV (FD1, FD4) vs. ostrich hindlimb digits I, II, and V (HD1, HD2, HD5). The circle adjacent to HD3 represents the gene number responsible for the adaptation of ostrich hindlimb digit III (HD3). The schematic illustrations of adult digits are based on the anatomical descriptions in (Delfino et al. 2010; de Bakker et al. 2013; Gregorovičová et al. 2018).

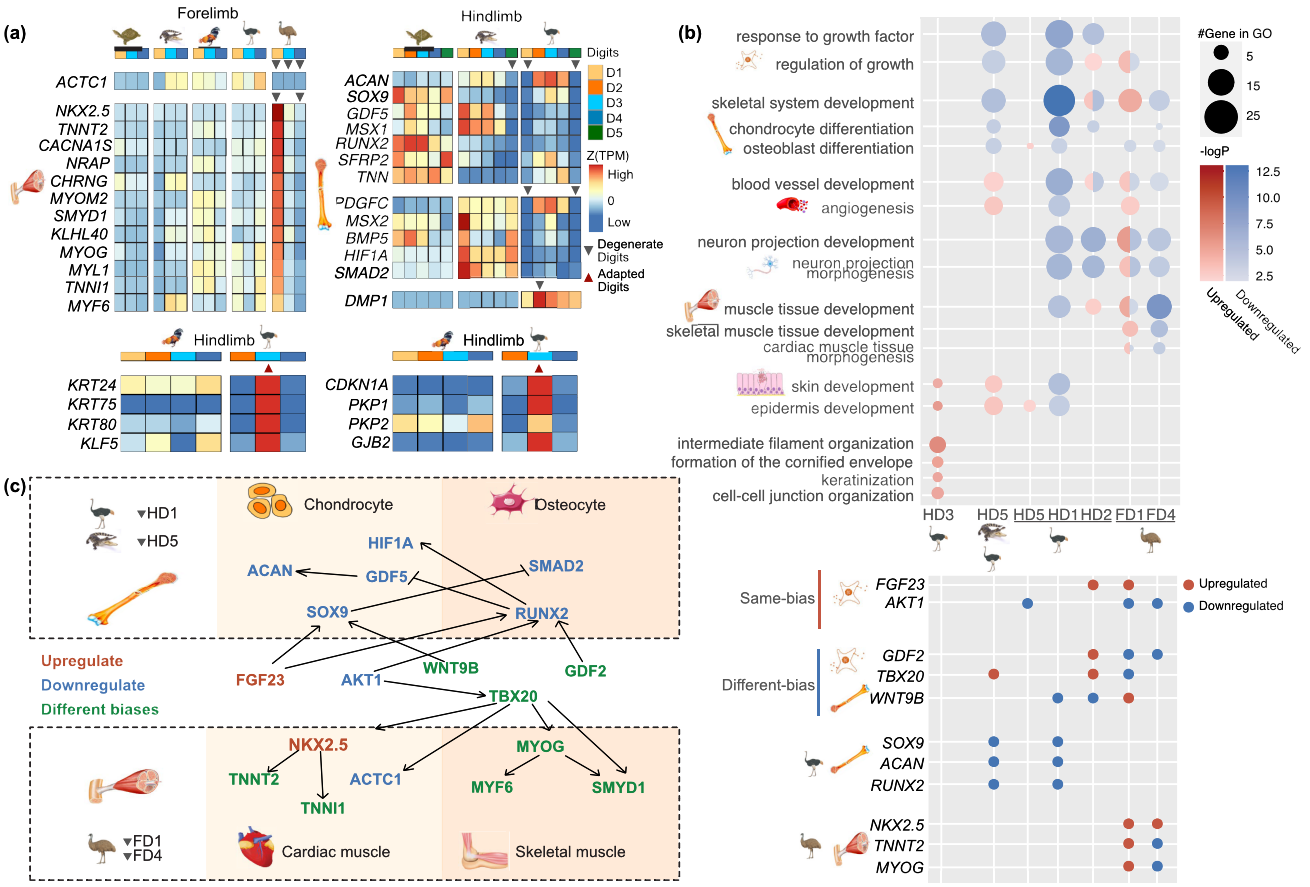

Figure 2 Candidate genes for the degenerating or adaptively evolving ratite digits. a) The normalized expression of the genes with reported muscle-related functions in the emu forelimb digits in HH28, skeletal-related functions in the ostrich hindlimb digits in HH28, and epidermal-related functions in the ostrich hindlimb digits in HH40. The different triangles mark the degenerated digits (down triangles) or adaptively evolving digits (up triangles). b) The upper panel shows the Gene Ontology (GO) enrichment patterns of candidate responsible genes for each digit that undergoes degeneration or adaptive evolution in each species. The circle size is scaled to the number of candidate genes of respective GO terms (shown in the *y*-axis, different GO terms are grouped into neuron, skeleton, muscle, and skin development, shown by icons) corresponding to each digit (*x*-axis). The circle color is scaled to the negative log10 *P*-value according to the hypergeometric test, with the blue color showing the downregulated genes, and the red color showing the upregulated genes compared to the homologous digits of other species. The lower panel shows the trend of expression changes of some example genes in each GO term shared among different degenerating digits. c) Different gene regulatory networks (Iwamoto et al. 2013; Cruet-Hennequart et al. 2015; Deng et al. 2015; Hinds et al. 2016; Chavez et al. 2017; Imran et al. 2017; Ganassi et al. 2018; Valenti et al. 2018; Kwon et al. 2020; Dalle Carbonare et al. 2022) are involved in the degeneration of ostrich/crocodile HD5 and emu forelimb FD1/4. The few shared genes are shown between the upper and lower panels, and gene names are colored for either being upregulated (red), downregulated (blue), or showing different trends of regulation between digits (green).

(brachydactyly) and malformed digits (Buxton et al. 2001; Byrnes et al. 2010; Ryoo et al. 2010; Gibson and Briggs 2016; Dateki 2017; Csukasi et al. 2019; Lefebvre et al. 2019).

By contrast, fewer than 3% of the candidate genes for the degenerating emu forelimb digit 1, 4 (FD1,4) and ostrich HD1,2,5 are shared, and the same candidate genes or genes of the same GO terms often show opposite changes of gene expression between different digits (Fig. 2b), indicating independently evolved emu wing and ostrich foot digit degeneration after the divergence of the 2 species (Fig. 1). The few shared genes include the growth factor *Fgf23* that is upregulated in the ostrich HD2 and emu FD1 relative to other digits of the same species. Its overexpression in mice leads to impaired bone mineralization and muscle weakness (Lu and Feng 2011; Si et al. 2021). And *Akt1*, a key regulator of osteoblast and osteoclast activity, is downregulated in ostrich HD5 and emu FD1/4. The disruption of this gene in mice produces dwarfism and reduced ossification of cartilage (Cho et al. 2001; Kawamura et al. 2007; Fukai et al. 2010). Several other shared genes however show opposite patterns of expression changes between emu and ostrich in the degenerating digits, such as the growth factors *Gdf2* and *Tbx20* (Kirk et al. 2007; Hodgson et al. 2020) and the gene *Wnt9b,* all of which are reported to be critical for skeleton or muscle development (Lan et al. 2006) (Fig. 2b, Figure S3).

Overall the degeneration of emu wing digits predominantly involves pathways of muscle development, while that of ostrich feet digits involves mainly downregulation of many skeletal development genes, according to their contrasting gene numbers and significance levels of the enriched GO terms of skeleton or muscle development pathways (Fig. 2c). The pattern of emu is consistent with a recent study of emu embryonic wings of earlier stages, which attributed the wing degeneration to immobilization of

wing buds caused by cell death and differentiation arrest of muscle progenitor cells into autopodial muscle (Tsuboi et al. 2024). The cardiac muscle development TF *Nkx2.5* was reported to be abnormally activated in the emu wing bud (Farlie et al. 2017), and we found here it is also upregulated in all the emu digits relative to their homologs of other species (Fig. 2a). Interestingly, its downstream gene *Tnnt2* (Wei and Jin 2016) is upregulated in the emu degenerating wing digit 1, but downregulated in the digit 4 compared to other birds, and we confirmed this with whole mount RNA in situ hybridization (Figure S4). The similar opposite expression changes between D1 and D4 have been observed for other cardiac (e.g. *Tnn1*) and skeletal (e.g. *Myog*) muscle development genes (Fig. 2a). In fact, the candidate genes annotated with muscle development GO terms are more often upregulated in the emu wing D1, but downregulated in the emu wing D4 (Fig. 2a and Figure S5). These results together show that even for the same species, different digits can have different mechanisms of degeneration, possibly influenced by their different identities related to the AP positions. Although previous works reported apoptosis with a TUNEL assay in the chicken wing digit 4 (de Bakker et al. 2021), we did not observe a significant (Wilcoxon test, $P < 0.05$) upregulation of apoptosis-related marker genes in the degenerating digits relative to the retained digits in most of the studied species, except for an upregulation of *Bak1* in the emu FD1, and *Apaf1* in the crocodile HD5 (Figure S6).

To characterize the expression signatures of adaptive evolution in ostrich HD3, we compared gene expression between each ostrich and chicken hindlimb digits across 5 (HH28 to HH40) corresponding developmental stages, and identify differentially expressed genes (DEGs) specific to HD3 (Materials and Methods, Figure S7). Almost all HD3-specific DEGs were found at stage 40 and exhibit an upregulation of transcription relative to their chicken orthologs. And they seem to involve few genes of skeletal and muscle development. Instead, GO analysis indicated that they are enriched for "intermediate filament organization", "formation of the cornified envelope", and "cell-cell junction organization" (Fig. 2b). By stage HH40, we found upregulation of many epidermal-related genes. Those genes comprise core structural keratins and cornification regulators (e.g. *Krt24, Krt75, Krt80* (Ho et al. 2022)), master transcription factors directing keratinocyte differentiation (e.g. *Klf5, Cdkn1a* (Kreis et al. 2019; Lyu et al. 2022)), and critical intercellular junction stabilizers essential for withstanding high mechanical stress (e.g. *Pkp1, Pkp2, Gjb2* (Richard 2001; Iossa et al. 2011; Rietscher et al. 2016)). This is consistent with the reported thicker epidermis and extra toepad structure of this digit relative to the only other retained HD4 and homologous digits of other species (El-Gendy et al. 2012), for protecting the soft tissue and absorbing the concussion during walking and running.

In conclusion, our results provide molecular evidence consistent with developmental patterns and the morphological reduction of hindlimb digit V described in basal dinosaurs and their relatives (Sereno and Novas 1992; Sereno 2012). Paleognaths have long captivated evolutionary biologists as a classic model for debating biogeographical vicariance versus convergent evolution, specifically regarding whether flightlessness was a single ancient event or evolved independently. Consistent with the phylogenomic consensus supporting multiple independent losses (Harshman et al. 2008; Widrig et al. 2025), we found that the emu and ostrich evolved independent modifications to their wings or feet, involving different skeletal or muscle developmental genes in the degenerating digits. While the ostrich specifically in one hindlimb digit with expression changes in genes of epidermal development and cell adhesion to adapt for running.

Methods and materials

Data collection

All of the animal embryos were sampled after approval from the Laboratory Animal Welfare and Ethics Committee of Zhejiang University. For the three birds, fertilized chicken (White Leghorns), emu, and ostrich eggs were obtained from farms nearby Hangzhou, Lishui, and Xi'An, and the eggs were incubated at 37.5, 36.5, and 37 °C, respectively, with a humidity around 65% to 75%. We collected the samples at Hamburger and Hamilton stage 28 and stage 32 embryos (Hamburger and Hamilton 1992; Brand et al. 2017). The hindlimb shape was used as a morphological criterion to stage embryos, with the Hamburger-Hamilton stage for chickens and also for emu and ostrich embryos. Stage 28 (we defined it as an early digit stage) featured a second digit and third toe longer than the others, creating a pointed contour in the digital and toe plates. By stage 32 (we defined it as a late digit stage), all digits and toes have significantly lengthened, with thin, concave-webbed structures forming between them. Corresponding stages of other vertebrate species were chosen according to the similarity of their digit morphology with that of the chicken. We did not collect the samples of hindlimb digit 5 of the chicken, and digits 1 and 5 of the emu, because they are barely detectable during dissections (Figure S8). We also collected cartilage or boned individual digits of chicken hindlimb D1 to D4, and ostrich hindlimb D2, D3, and D4, in stage 36, stage 38, and stage 40 stages according to their embryonic morphology (Hamburger and Hamilton 1992; Bai et al. 2023), for the Alcian blue/alizarin red staining and following analysis on the degeneration of hindlimb D2 and the adaptive evolution of hindlimb D3 in ostrich. We collected the Chinese softshell turtle eggs from a farm nearby Hangzhou, and incubated them at 30 °C. We collected limb bud and digit samples on 18 and 28 days according to the staging work of (Tokita and Kuratani 2001). We collected the Siamese crocodile eggs from a farm in Beihai and incubated them at 33 °C. The samples were collected on 24 and 31-33 days according to the staging work of Ferguson (1985). For all samples, we collected each digit, including its posterior interdigital mesoderm from the forelimb and hindlimb, respectively. Left and right digit samples were collected as replicates from the same individual and placed immediately in the RNAlater (Sigma-Aldrich) solution. RNA was extracted from each sample with TRIzol (Thermo Fisher Scientific) (Chomczynski and Mackey 1995). Then, paired-end libraries were constructed using NEBNext UltraTM RNA Library Prep Kit for Illumina (NEB, USA), and 2Gb paired-end reads of 150 bp long were produced for each library. We also collected additional forelimb and hindlimb samples and fixed them in ethanol overnight for Alcian staining. The samples were then transferred to acetone overnight. Alcian blue and alizarin red staining were performed for 1 to 2 days. Embryos were cleared with 1% KOH, then placed in 50% glycerol/KOH solution until transparent, and finally transferred to 100% glycerol for long-term storage (Ovchinnikov 2009).

Read mapping and analysis of gene expression

We used the genomes of chicken genome (GRCg6a,GCA_000002315.5), emu (ZJU2, GCA_016128335.2), ostrich (ASM69896v1, GCA_000698965.1), Australian saltwater crocodile (CroPor_comp1, GCA_001723895.1, which is the closest-related species with available genome to Siamese crocodile), Chinese softshell turtle (PelSin_1.0, GCA_000230535.1) as reference for aligning the RNA-seq reads with *HISAT2* (2.1.0) (Kim et al. 2019). The alignment rates between the RNA-seq reads vs. the reference genomes range between 70% and 90%. Raw gene counts were counted by *featureCounts*(v2.0.1) and normalized by transcripts per million (TPM) method for estimating the gene expression level.

Identification of candidate responsible genes

We define MFGs as those that are upregulated or downregulated relative to the rest of the digits in either of the sampled developmental stages. The upregulation or downregulation index was measured by $\frac{\sum_{i=1}^{n} 1-\widehat{x_i}}{n-1}$; $\widehat{x_i} = \frac{x_i}{max_{1\le i\le n}(x_i)}$ or $\frac{\sum_{i=1}^{n} 1-\widehat{x_i}}{1-n}$; $\widehat{x_i} = \frac{1}{m_{1\le i\le n}(x_i)}$ according to Kryuchkova-Mostacci and Robinson-Rechavi (2017), where x is the TPM of the respective digit, and n is the tissue number. A value higher than 0.5 was used as the cutoff for defining MFGs according to the distribution of the index values of each species. We inferred the fast change in expression genes related to digit degeneration, with expression changes in the emu forelimb (D1, D4), ostrich hindlimb (D1, D5), and crocodile hindlimb (D5) by *PhyDGET* [https://www.github.com/peaselab/phydget] (Pease et al. 2022). We first normalized and transformed the RNA-seq read counts of the digits of each species into log2(cpm) (log2 transform of counts per million), then tested the expression difference across seven species using *BayesTrait* (v3.0.2) (Pagel et al. 2004) under a null model that hypothesizes constant rate changes and alternative models. Marginal log-likelihoods were compared to calculate the Bayes factors, which improved the alternative model fit. And the genes can be defined with species- or branch-specific changes of expression levels relative to their orthologs in outgroups. For the putative adaptively evolving genes of the ostrich HD3, we performed differential expression analysis using *DESeq2* (Love et al. 2014) by constructing a combined grouping factor encompassing species and digit to model the orthologous gene counts. Specifically, for each matched stage from HH28 to HH40, genes were defined as ostrich HD3-biased only if they simultaneously fit 2 criteria: (1) exhibiting significant differential expression in the ostrich HD3 compared to both digits (HD2 and HD4); and (2) exhibiting significant differential expression in the ostrich HD3 compared to the homologous chicken HD3 at the identical stage. We use a threshold of $|\log2(\text{FoldChange})| > 1$ and adjusted P-value < 0.05.

Gene ontology (GO) term analysis

The GO enrichments were produced by *Metascape* (Zhou et al. 2019), and the orthologous genes to mouse for digit degeneration were provided to this online tool. All genes in the genome were used as the enrichment background.

Whole mount in situ hybridization

RNA was extracted from a HH28 chicken limb as described earlier, and cDNA was synthesized using the High-Capacity cDNA Reverse Transcription kit. PCR products were purified and cloned into the *pSPT19* vector using the ClonExpress Ultra One Step Cloning Kit (Vazyme). Vectors were transformed into DH5α competent cells. Sense and antisense probes were generated by linearizing plasmids transcribed with T7 polymerase. Probes, labeled with digoxigenin (Sigma–Aldrich), were hybridized with chicken, emu, and ostrich embryos at 70 °C. The in situ hybridization method followed the GEISHA Project of Whole Mount In Situ Hybridization Protocol for mRNA Detection [http://geisha.arizona.edu/].

Supplementary material

Supplementary material is available at *Molecular Biology and Evolution* online.

Funding

Qi Zhou is supported by the National Key Research and Development Program of China (2023YFA1800500, 2024YFA1802500), National Natural Science Foundation of China (32170415), and Fundamental Research Funds for the Central Universities (226-2024-00055) from Zhejiang University.

Conflicts of Interest

None declared.

Data availability

The RNA-seq data generated in this work for turtle, crocodile, chicken, emu and ostrich are available in the NCBI Sequence Read Archive (SRA) database under the BioProject accession number PRJNA1258050.

Code availability

Scripts for analyzing data and plot figures are available on GitHub at https://github.com/KangWwen/Digit-Degeneration/

References

Abourachid A. Bipedalism in birds, a determining feature for their adaptive success. *J Soc Biol*. 2006:200:169–175. https://doi.org/10.1051/jbio:2006018.

Bai S *et al.* Comparison of embryonic development, from HH21 to HH40, between ostrich (*Struthio camelus*) and chicken (*Gallus gallus*). *Dev Dyn*. 2023:252:668–681. https://doi.org/10.1002/dvdy.568.

Botelho JF *et al.* Skeletal plasticity in response to embryonic muscular activity underlies the development and evolution

of the perching digit of birds. *Sci Rep*. 2015:5:9840. https://doi.org/10.1038/srep09840.

Botelho JF, Smith-Paredes D, Nunez-Leon D, Soto-Acuna S, Vargas AO. The developmental origin of zygodactyl feet and its possible loss in the evolution of Passeriformes. *Proc Biol Sci*. 2014:281:20140765. https://doi.org/10.1098/rspb.2014.0765.

Brand Z, Cloete SWP, Malecki IA, Brown CR. Ostrich (*Struthio camelus*) embryonic development from 7 to 42 days of incubation. *Br Poult Sci*. 2017:58:139–143. https://doi.org/10.1080/00071668.2016.1259529.

Buxton P, Edwards C, Archer CW, Francis-West P. Growth/differentiation factor-5 (GDF-5) and skeletal development. *J Bone Joint Surg Am*. 2001:83-A Suppl 1:S23–S30. https://doi.org/10.2106/00004623-200100001-00004.

Byrnes AM *et al.* Mutations in GDF5 presenting as semidominant brachydactyly A1. *Hum Mutat*. 2010:31:1155–1162. https://doi.org/10.1002/humu.21338.

Chavez RD, Coricor G, Perez J, Seo HS, Serra R. SOX9 protein is stabilized by TGF-β and regulates PAPSS2 mRNA expression in chondrocytes. *Osteoarthritis Cartilage*. 2017:25:332–340. https://doi.org/10.1016/j.joca.2016.10.007.

Cho H, Thorvaldsen JL, Chu Q, Feng F, Birnbaum MJ. Akt1/PKBalpha is required for normal growth but dispensable for maintenance of glucose homeostasis in mice. *J Biol Chem*. 2001:276:38349–38352. https://doi.org/10.1074/jbc.C100462200.

Chomczynski P, Mackey K. Short technical reports. Modification of the TRI reagent procedure for isolation of RNA from polysaccharide- and proteoglycan-rich sources. *Biotechniques*. 1995:19:942–945.

Cooper KL *et al.* Patterning and post-patterning modes of evolutionary digit loss in mammals. *Nature*. 2014:511:41–45. https://doi.org/10.1038/nature13496.

Cruet-Hennequart S *et al.* Radiation-induced alterations of osteogenic and chondrogenic differentiation of human mesenchymal stem cells. *PLoS One*. 2015:10:e0119334. https://doi.org/10.1371/journal.pone.0119334.

Csukasi F *et al.* Dominant-negative SOX9 mutations in campomelic dysplasia. *Hum Mutat*. 2019:40:2344–2352. https://doi.org/10.1002/humu.23888.

Dalle Carbonare L *et al.* Modulation of miR-204 expression during chondrogenesis. *Int J Mol Sci*. 2022:23:2130. https://doi.org/10.3390/ijms23042130.

Dateki S. ACAN mutations as a cause of familial short stature. *Clin Pediatr Endocrinol*. 2017:26:119–125. https://doi.org/10.1297/cpe.26.119.

de Bakker MAG *et al.* Digit loss in archosaur evolution and the interplay between selection and constraints. *Nature*. 2013:500:445–448. https://doi.org/10.1038/nature12336.

de Bakker MAG *et al.* Selection on phalanx development in the evolution of the bird wing. *Mol Biol Evol*. 2021:38:4222–4237. https://doi.org/10.1093/molbev/msab150.

Delfino M, Fritz U, Sánchez-Villagra MR. Evolutionary and developmental aspects of phalangeal formula variation in pig-nose and soft-shelled turtles (*Carettochelyidae* and *Trionychidae*). *Org Divers Evol*. 2010:10:69–79. https://doi.org/10.1007/s13127-010-0019-x.

Deng L *et al.* Inhibition of FOXO1/3 promotes vascular calcification. *Arterioscler Thromb Vasc Biol*. 2015:35:175–183. https://doi.org/10.1161/ATVBAHA.114.304786.

El-Gendy SAA, Derbalah A, El-Magd MERA. Macro-microscopic study on the toepad of ostrich (*Struthio camelus*). *Vet Res Commun*. 2012:36:129–138. https://doi.org/10.1007/s11259-012-9522-1.

Farlie PG *et al.* Co-option of the cardiac transcription factor Nkx2.5 during development of the emu wing. *Nat Commun*. 2017:8:132. https://doi.org/10.1038/s41467-017-00112-7.

Feduccia A, Nowicki J. The hand of birds revealed by early ostrich embryos. *Naturwissenschaften*. 2002:89:391–393. https://doi.org/10.1007/s00114-002-0350-y.

Ferguson MWJ. The reproductive biology and embryology of the crocodilians. *Biol Reptilia*. 1985:14:329–491. https://biostor.org/reference/110202.

Fukai A *et al.* Akt1 in murine chondrocytes controls cartilage calcification during endochondral ossification under physiologic and pathologic conditions. *Arthritis Rheum*. 2010:62:826–836. https://doi.org/10.1002/art.27296.

Ganassi M *et al.* Myogenin promotes myocyte fusion to balance fibre number and size. *Nat Commun*. 2018:9:4232. https://doi.org/10.1038/s41467-018-06583-6.

Gatesy SM. Handbook of avian anatomy: nomina Anatomica Avium. *Condor*. 1995:97:849–850. https://doi.org/10.2307/1369201.

Gauthier J. Saurischian monophyly and the origin of birds. *Mem Calif Acad Sci*. 1986:8:1–55. https://biostor.org/reference/110202.

Gibson BG, Briggs MD. The aggrecanopathies; an evolving phenotypic spectrum of human genetic skeletal diseases. *Orphanet J Rare Dis*. 2016:11:86. https://doi.org/10.1186/s13023-016-0459-2.

Gregorovičová M, Kvasilová A, Sedmera D. Ossification pattern in forelimbs of the siamese crocodile (*Crocodylus siamensis*): similarity in ontogeny of carpus among crocodylian Species. *Anat Rec*. 2018:301:1159–1168. https://doi.org/10.1002/ar.23792.

Hamburger V, Hamilton HL. A series of normal stages in the development of the chick embryo. *Dev Dyn*. 1992:195:231–272. https://doi.org/10.1002/aja.1001950404.

Harshman J *et al.* Phylogenomic evidence for multiple losses of flight in ratite birds. *Proc Natl Acad Sci U S A*. 2008:105:13462–-13467. https://doi.org/10.1073/pnas.0803242105.

Hinds TD *et al.* Overexpression of glucocorticoid receptor β enhances myogenesis and reduces catabolic gene expression. *Int J Mol Sci*. 2016:17:232. https://doi.org/10.3390/ijms17020232.

Ho M *et al.* Update of the keratin gene family: evolution, tissue-specific expression patterns, and relevance to clinical disorders. *Hum Genomics*. 2022:16:1. https://doi.org/10.1186/s40246-021-00374-9.

Hodgson J *et al.* Characterization of GDF2 mutations and levels of BMP9 and BMP10 in pulmonary arterial hypertension. *Am J Respir Crit Care Med*. 2020:201:575–585. https://doi.org/10.1164/rccm.201906-1141OC.

Imran M *et al.* Mangiferin: a natural miracle bioactive compound against lifestyle related disorders. *Lipids Health Dis*. 2017:16:84. https://doi.org/10.1186/s12944-017-0449-y.

Iossa S, Marciano E, Franzé A. GJB2 gene mutations in syndromic skin diseases with sensorineural hearing loss. *Curr Genomics*.

2011:12:475–785. https://doi.org/10.2174/138920211797904098.

Iwamoto M, Ohta Y, Larmour C, Enomoto-Iwamoto M. Toward regeneration of articular cartilage. *Birth Defects Res C Embryo Today*. 2013:99:192–202. https://doi.org/10.1002/bdrc.21042.

Kawamura N *et al.* Akt1 in osteoblasts and osteoclasts controls bone remodeling. *PLoS One*. 2007:2:e1058. https://doi.org/10.1371/journal.pone.0001058.

Kim D, Paggi JM, Park C, Bennett C, Salzberg SL. Graph-based genome alignment and genotyping with HISAT2 and HISAT-genotype. *Nat Biotechnol*. 2019:37:907–915. https://doi.org/10.1038/s41587-019-0201-4.

Kirk EP *et al.* Mutations in cardiac T-box factor gene TBX20 are associated with diverse cardiac pathologies, including defects of septation and valvulogenesis and cardiomyopathy. *Am J Hum Genet*. 2007:81:280–291. https://doi.org/10.1086/519530.

Kreis NN, Louwen F, Yuan J. The multifaceted p21 (Cip1/Waf1/CDKN1A) in cell differentiation, migration and cancer therapy. *Cancers (Basel).* 2019:11:1220. https://doi.org/10.3390/cancers11091220.

Kryuchkova-Mostacci N, Robinson-Rechavi M. A benchmark of gene expression tissue-specificity metrics. *Brief Bioinform*. 2017:18:205–214. https://doi.org/10.1093/bib/bbw008.

Kundrát M. Primary chondrification foci in the wing basipodium of *Struthio camelus* with comments on interpretation of autopodial elements in Crocodilia and Aves. *J Exp Zool B Mol Dev Evol*. 2009:312:30–41. https://doi.org/10.1002/jez.b.21240.

Kwon DH, Ryu J, Kim YK, Kook H. Roles of histone acetylation modifiers and other epigenetic regulators in vascular calcification. *Int J Mol Sci*. 2020:21:3246. https://doi.org/10.3390/ijms21093246.

Lan Y *et al.* Expression of Wnt9b and activation of canonical Wnt signaling during midfacial morphogenesis in mice. *Dev Dyn*. 2006:235:1448–1454. https://doi.org/10.1002/dvdy.20723.

Lefebvre V, Angelozzi M, Haseeb A. SOX9 in cartilage development and disease. *Curr Opin Cell Biol*. 2019:61:39–47. https://doi.org/10.1016/j.ceb.2019.07.008.

Love MI, Huber W, Anders S. Moderated estimation of fold change and dispersion for RNA-Seq data with DESeq2. *Genome Biol*. 2014:15:550. https://doi.org/10.1186/s13059-014-0550-8.

Lu Y, Feng JQ. FGF23 in skeletal modeling and remodeling. *Curr Osteoporos Rep*. 2011:9:103–108. https://doi.org/10.1007/s11914-011-0053-4.

Lyu Y *et al.* KLF5 governs sphingolipid metabolism and barrier function of the skin. *Genes Dev*. 2022:36:822–842. https://doi.org/10.1101/gad.349662.122.

Ovchinnikov D. Alcian blue/alizarin red staining of cartilage and bone in mouse. *Cold Spring Harb Protoc*. 2009:2009:db.prot5170. https://doi.org/10.1101/pdb.prot5170.

Pagel M, Meade A, Barker D. Bayesian estimation of ancestral character states on phylogenies. *Syst Biol*. 2004:53:673–684. https://doi.org/10.1080/10635150490522232.

Pease J *et al.* Layered evolution of gene expression in "superfast" muscles for courtship. *Proc Natl Acad Sci U S A*. 2022:119:e2119671119. https://doi.org/10.1073/pnas.2119671119.

Raikow RJ. Locomotor system. In: King AS, McLelland J, editors. *Form and function in birds*. Academic Press; 1985. p. 57–147.

Richard G. Connexin disorders of the skin. *Adv Dermatol*. 2001:17:243–277. https://doi.org/10.1016/j.clindermatol.2004.09.010.

Rietscher K *et al.* Growth retardation, loss of desmosomal adhesion, and impaired tight junction function identify a unique role of plakophilin 1 in vivo. *J Invest Dermatol*. 2016:136:1471–1478. https://doi.org/10.1016/j.jid.2016.03.021.

Ryoo HM, Kang HY, Lee SK, Lee KE, Kim JW. RUNX2 mutations in cleidocranial dysplasia patients. *Oral Dis*. 2010:16:55–60. https://doi.org/10.1111/j.1601-0825.2009.01623.x.

Schaller NU, D'Août K, Villa R, Herkner B, Aerts P. Toe function and dynamic pressure distribution in ostrich locomotion. *J Exp Biol*. 2011:214:1123–1130. https://doi.org/10.1242/jeb.043596.

Sereno PC. Taxonomy, morphology, masticatory function and phylogeny of heterodontosaurid dinosaurs. *Zookeys*. 2012:226:1–225. https://doi.org/10.3897/zookeys.226.2840.

Sereno PC, Novas FE. The complete skull and skeleton of an early dinosaur. *Science*. 1992:258:1137–1140. https://doi.org/10.1126/science.258.5085.1137.

Si Y *et al.* FGF23, a novel muscle biomarker detected in the early stages of ALS. *Sci Rep*. 2021:11:1–12. https://doi.org/10.1038/s41598-021-91496-6.

Stewart TA *et al.* Evidence against tetrapod-wide digit identities and for a limited frame shift in bird wings. *Nat Commun*. 2019:10:3244. https://doi.org/10.1038/s41467-019-11215-8.

Tokita M, Kuratani S. Normal embryonic stages of the Chinese softshelled turtle *Pelodiscus sinensis* (*Trionychidae*). *Zool Sci*. 2001:18:705–715. https://doi.org/10.2108/zsj.18.705.

Tsuboi E *et al.* Immobilization secondary to cell death of muscle precursors with a dual transcriptional signature contributes to the emu wing skeletal pattern. *Nat Commun*. 2024:15:1–14. https://doi.org/10.1038/s41467-024-52203-x.

Valenti MT, Dalle Carbonare L, Mottes M. Ectopic expression of the osteogenic master gene RUNX2 in melanoma. *World J Stem Cells*. 2018:10:78–81. https://doi.org/10.4252/wjsc.v10.i7.78.

Wang Z, Young RL, Xue H, Wagner GP. Transcriptomic analysis of avian digits reveals conserved and derived digit identities in birds. *Nature*. 2011:477:583–586. https://doi.org/10.1038/nature10391.

Wei B, Jin JP. TNNT1, TNNT2, and TNNT3: isoform genes, regulation, and structure-function relationships. *Gene*. 2016:582:1–13. https://doi.org/10.1016/j.gene.2016.01.006.

Widrig K, Alfieri F, Kuo P-C, James H, Field DJ. Quantitative analysis of stem-palaeognath flight capabilities sheds light on ratite dispersal and flight loss. *Biol Lett*. 2025:21:20250320. https://doi.org/10.1098/rsbl.2025.0320.

Young JJ, Grayson P, Edwards SV, Tabin CJ. Attenuated Fgf signaling underlies the forelimb heterochrony in the Emu *Dromaius novaehollandiae*. *Curr Biol*. 2019:29:3681–3691.e3685. https://doi.org/10.1016/j.cub.2019.09.014.

Zhou Y *et al.* Metascape provides a biologist-oriented resource for the analysis of systems-level datasets. *Nat Commun*. 2019:10:1523. https://doi.org/10.1038/s41467-019-09234-6.